Functionalization of Ag nanoparticles with the bis-acridinium lucigenin as a chemical assembler in the detection of persistent organic pollutants by surface-enhanced Raman scattering

L. Guerrini[a], *A.E. Aliaga*[b], *J. Cárcamo*[b], *J.S. Gómez-Jeria*[b], *S. Sanchez-Cortes*[a,*], *M.M. Campos-Vallette*[b], *J.V. García-Ramos*[a]

[a] *Instituto de Estructura de la Materia CSIC, Serrano 121, 28006 Madrid, Spain*
[b] *University of Chile, Faculty of Sciences, PO Box 653, Santiago, Chile*

A B S T R A C T

Organochlorine pesticide endosulfan has been detected for the first time by using surface-enhanced Raman scattering (SERS) at trace concentrations. The bis-acridinium dication lucigenine was successfully used as a molecular assembler in the functionalization of metal nanoparticles to facilitate the approach of the pesticide to the metal surface. From the SERS spectra valuable information about the interaction mechanism between the pesticide and lucigenin can be deduced. In fact, endosulfan undergoes an isomerization upon adsorption onto the metal, while the viologen undergoes a rotation of the acridinium planes to better accommodate the pesticide molecule. An interaction between the N atom of the central acridinium ring and the pesticide Cl–C=C–Cl fragment is verified through a charge-transfer complex. The present study affords important information which can be applied to the design of chemical sensor systems of persistent organic pollutants based on the optical detection on functionalized metal nanoparticle.

Keywords:
Metal functionalization
Viologen
Lucigenin
Molecular recognition
Surface-enhanced Raman scattering
Nanosensors
Organochlorine pesticides

1. Introduction

The functionalization of metal nanoparticle (NP) surfaces for chemical sensing is a topic of maximum interest nowadays [1,2]. An special application of functionalized nanoparticles has been performed in the field of the surface-enhanced Raman scattering (SERS) [3–5] technique. SERS is an analytical technique with a high sensitivity, based on the giant electromagnetic enhancement (EM) derived from localized plasmon resonance (LPR) in metal nanoparticles, leading to the intensification of the Raman emission. SERS can be successfully applied in the identification and most probable orientation of molecules adsorbed onto a surface [6]. The enhancement of the Raman signal induced by nanostructured metal surfaces can take place through two different mechanisms: electromagnetic enhancement, and charge-transfer (CT) [7–10]. The last mechanism is not so important under the viewpoint of the signal intensification but has an influence on the spectral pattern of the SERS spectra [11]. In both cases the probe molecule has to be close enough to the surface as to undergo

* *Corresponding author*. Tel.: +34 915 616800; fax: +34 915 645557.
E-mail address: imts158@iem.cfmac.csic.es (S. Sanchez-Cortes).

a significant Raman intensification by SERS, because of the short-range effect of both mechanisms. Unfortunately, many compounds of interest are SERS inactive due to their inability to approach the metal surface. This is the case of many persistent organic pollutants (POPs). In spite of this fact, Alak and Vodinh reported the first SERS spectra of some chlorinated pesticides [12,13], where the presence of active functional groups seemed to be favorable to induce the necessary approach of the analyte to the metal surface. However, pesticides containing a high amount of chlorine atoms are highly inactive in SERS and cannot be directly detected by SERS due to the lack of affinity to the metal.

In the last years we have demonstrated that intense SERS spectra can be obtained from polycyclic aromatic hydrocarbons (PAHs), a special group of POPs which are also inactive in SERS, by changing the metal surface affinity with an appropriate functionalization with host molecules such as calixarenes or nanotubes [14–17] and humic acids [18]. The host molecule required a double functionality: it must bind the metal and interact with the analyte bringing it closer to the metal surface.

Bipyridinium dications (BIPs), also known as viologen compounds, display an interesting electrochemical behavior which makes them useful systems in a wide range of applications [19]. For instance, they have been used as electroactive materials in the functionalization of metal electrodes for sensing methods [20–22]. Among the BIPs cations, lucigenin (*N*,*N*′-dimethyl-9,9′-biacridinium dinitrate, LG, Fig. 1) is an interesting viologen compound employed so far in chloride or glucose sensing [23–25], thus, it could be used in the functionalization of metal surfaces for the detection of other compound of interest, such as POPs.

In previous works we have demonstrated that LG can attach strongly a metal surface in the presence of anions of different nature in the medium [26,27]. The presence of halides is important to ensure the interaction of quaternary ammines onto the metal surface [28,29]. In a recent work we have reported that the interaction of LG with the Ag–Cl system is so strong that a charge-transfer complex is taking place [30].

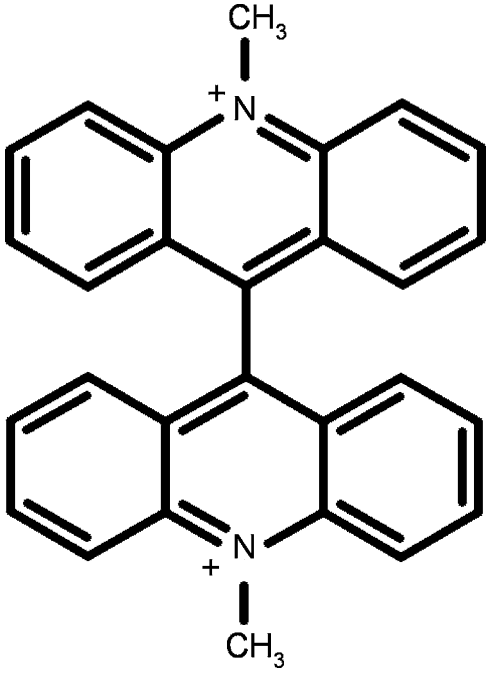

Fig. 1 – Structure of lucigenine dication (LG).

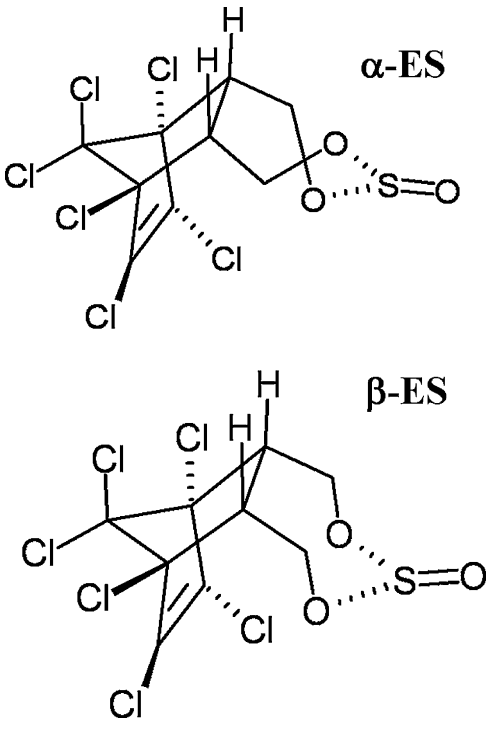

Fig. 2 – Structures of α- and β-endosulfan.

In the present work we have checked the sensing ability of Ag nanoparticles (Ag NPs) functionalized by LG using as probe molecule the organochlorine insecticide endosulfan (ES, Fig. 2). This compound is frequently used in agricultural practices and can be bioaccumulated in the food chain, displaying a high toxicity [31]. Endosulfan belongs to the insecticide/acaricide class type containing a double bond, several C–Cl bonds and a sulfonic ester. ES develops its toxicity mainly on the nerve cell membranes, by inhibiting the transport of cations as Ca^{2+}, K^{+}, Na^{+} and Mg^{2+} across the membranes [32–34]. It is possible to distinguish two main moieties within their structures: the chlorinated part, which constitutes the active wedge of the molecule bringing the large excess of charge responsible for the interaction with electron receptors [35], and the sulfonic ester side, which acts as an anchor supporting the altering action of the pesticide [36]. The unchlorinated moiety strongly affects the relative toxicity of the insecticide and as a proof of that it is reported that the α-ES isomer (Fig. 2) displays much higher insecticidal property than the β-isomer [37].

In this work we propose a functionalization of Ag NPs with LG as a host molecule for the detection, by SERS, of low concentrations of the pesticide ES. To our knowledge no SERS spectra of ES have been reported so far, probably due to the fact that no SERS spectrum of this compound can be obtained in absence of molecular assemblers. Therefore, the SERS detection of this important pollutant can only be done by using a host molecule. Moreover, the detection and extraction of endosulfan by metal

nanoparticles Ag and Au have been performed by Nair et al. [38] by plasmon absorbance methods.

2. Experimental

2.1. Materials

Endosulfan (6,7,8,9,10,10-hexachloro-1,5,5a,6,9,9a-hexahydro-6,9-methane-2,4,3-benzodioxathiepyne-3-oxide) in versions α- and β-isomers was purchased from Aldrich and used as received. Stock solution of α-ES in ethanol was prepared to a final concentration of 10^{-3} M. LG dinitrate was purchased from Aldrich with a purity of >97% (w/w). Aqueous stock solutions of the compounds were prepared in Milli-Q water. All the reagents employed were of analytical grade.

2.2. Sample preparation

Colloidal silver nanoparticles were prepared by using hydroxylamine hydrochloride as reducing agent [39]. These nanoparticles exhibit the advantage of a more uniform distribution of size and shape together with the absence of interferences from the remainder oxidation products.

Samples for SERS measurements were prepared by adding first 10 μL of the α-ES solution to 1000 μL of the silver colloid and then 10 μL of a 10^{-4} M solution of the assembler LG. Then, the mixture was activated by addition of 20 μL of aqueous chloride 0.5 M up to a final concentration of 10^{-5} M. This activation is needed in order to increase the nanoparticles SERS activity by properly modifying the morphology of the particles. The effect of the Cl^- is double: it induces the aggregation of Ag colloid and promotes the adsorption of the assembler via a strong interaction with formation of an ionic pair or a CT complex, depending on the cases.

Finally, 500 μL of the final suspension was deposited onto a quartz cuvette and the scanning was performed at room temperature.

2.3. Instrumentation

The macro-SERS spectra were recorded with a Renishaw Raman RM2000 equipped with the 785 nm laser line, an electrically refrigerated CCD camera, and a notch filter to eliminate the elastic scattering. The spectra shown here were obtained by using a 30 mm focus length lens. The output laser power on the sample was about 2 mW. Spectral resolution was 4 cm^{-1}. The spectral scanning conditions are chosen to avoid sample degradation. The reported spectra were registered as single scans.

2.4. Assignment of bands

A bands assignment of α- and β-endosulfan in the solid was performed on the basis of general published data [40–42], as well as calculations of the IR and Raman spectra which will be published in the next future. A good agreement between experimental and calculated spectra was obtained. This result allowed us to confirm and complete the experimental bands assignment used in the discussion.

3. Results and discussion

3.1. SERS spectrum of lucigenin

The SERS spectrum of LG is shown in Fig. 3b compared to that of in aqueous solution (Fig. 3a). The main bands of these spectra as well as the assignments are shown in Table 1. The intensification of the in-plane C–C stretching bands at 1430 and 1395 cm^{-1} and the in-plane ring-breathing band at 1036 cm^{-1} indicate that LG is predominantly adsorbed through a perpendicular orientation onto the metal surface, according to the selection rules of SERS [6]. This is also corroborated by the intensification of bands at 668 and 419 cm^{-1} which can be attributed to skeletal vibrations involving the central part of the molecule bearing the N-CH_3 moiety [26]. On the other hand, the changes observed in the 1200–1300 cm^{-1} region, where bands corresponding to the inter-ring C–C stretching appear, suggest a possible rotation of the two acridinium planes around the main axe of LG (Fig. 1) upon adsorption on the metal.

The band at 1584 cm^{-1} is related to the central ring of the acridine moiety and indicates an interaction of LG with Cl^-, since this band is also observed in acridine at acidic pH, due to the protonation of the N atom, and also can be seen in CT complexes of acridine with adsorbed Cl^- ions on Ag colloids [29]. The changes observed in the Ag–Cl stretching band also

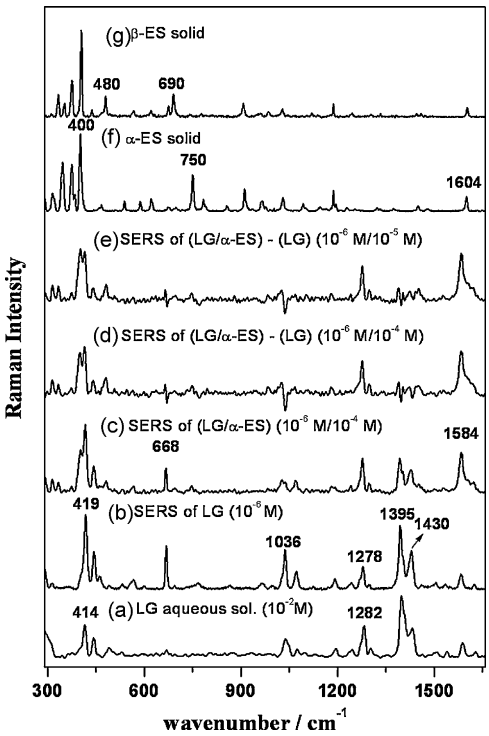

Fig. 3 – (a) Raman spectrum of LG in aqueous solution (10^{-2} M). (b) SERS spectrum of LG (10^{-6} M). (c) SERS spectrum of LG/α-ES complex (10^{-6} M/10^{-4} M). (d and e) SERS spectra of LG/α-ES complexes after subtraction of SERS of LG (spectrum b) at the concentration ratios: 10^{-6} M/10^{-5} M and 10^{-6} M/10^{-4} M, respectively. (f and g) Raman spectra of α-ES and β-ES isomers in the solid state.

Table 1 – Experimental IR, Raman and SERS bands (cm^{-1}) and the most probable bands assignment of LG and ES

LG in aqueous solution	SERS of LG	Assignments	α-ES	β-ES	SERS of α-ES	Assignments
			315m		315m	ν (C-Cl)
				333m	335m	
			345s	352m	351w	
			375s	375s	374w	
			400vs	403vs	400s	ν (C-Cl) linked to C=C
414s	419vs	δ(CCC), δ(CNC)				
443m	444s	Skeletal deformations		435w		Skeletal deformations
490w	490w		467w	479m	480w	
531w	531w		539w			
	564w		587m	566w	564w	
			621w	620w		
668w	668s	δ (CNC)	676w	690m	695w	
	767w	γ(C-H)	750s			
			784w			
	805w	γ(C-H)				
	966w	γ(C-H)	911m	907m		ν(C-H)
			966w	958w		
				986w		
1037m	1036w	ring breathing	1029w	1028w		
1074w	1070m	δ(C-H)				
1097w			1093w			
1195w	1191w	ν(N-CH_3)	1187m	1189vw	1181w	$\nu(SO_3)$
1245w	1244w	$\nu(C\text{-}C)_{i\text{-}r}$	1228w	1245vw	1240w	
1304w	1298w		1254w			
1400vs	1395vs	ν(C-C), ν(N-CH_3)				
1432s	1430s	ν(C-C), $\delta(CH_3)$	1450w	1459vw		$\delta(CH_2)$
1510w	1505w	ν(C=C)				
1539w	1535w	ν(C=C)				
1586m	1584m	ν(C=C), ν(C=N)	1604m	1602m		ν(C=C)
1628w	1624w	ν(C=C),ν(C=N)				

ν: stretching; δ: in-plain deformation; γ: out-of-plain deformation; $\nu_{i\text{-}r}$: inter-ring stretching.

corroborate the strong interaction between LG and chloride by the formation of a CT complex, and not simply by an ionic pair, as in the case of other amines [28]. The strong interaction of LG with this halide is further supported by the fact that this dication is used in the detection of Cl^-.

3.2. *Raman spectra of α- and β-ES isomers*

The Raman spectra of α-ES and β-ES are shown in Fig. 3f and g and a list of the main features and assignments is given in Table 1. As can be seen, the most intense Raman bands of solid

α-ES appear mainly in the region below 420 cm^{-1} (Fig. 3f), and are chiefly attributed to C–Cl stretching vibrations. The most intense feature among these bands is that appearing at ca. 400 cm^{-1}, which can be attributed to the C–Cl stretching of the Cl–C=C–Cl fragment, as indicated by our calculations and the evidences found here.

Other less intense bands are observed at 750 and 1604 cm^{-1}. The first one is assigned to a ring skeletal vibration coupled to C–Cl stretching motions. While, the second band is attributed to a C=C bond vibration. The weak bands observed around 1200 cm^{-1} could correspond to S=O stretching, while those between 900 and 1050 cm^{-1}, with a medium relative intensity, are attributed to CH deformations. Most of the bands appearing below 800 cm^{-1} are attributed to skeletal vibrations sensitive to the ES conformation, as revealed by comparison of the Raman spectra of α-ES and β-ES (Fig. 3f and g) in the solid. In particular, the band at 750 cm^{-1} in the α-ES isomer is dramatically affected, since it almost disappears in β-ES, while a medium band at 690 cm^{-1} appears. In addition, bands at 480 and 435 cm^{-1} are relatively intensified in the latter isomer. The structural region below 400 cm^{-1} is also sensitive to the conformational change: the band at 345 cm^{-1} disappears and two bands at 333 and 352 cm^{-1} appears instead. From the last result we have assigned these two bands to C–Cl stretching modes of the C atoms directly linked to the sulfonic ester group. All these changes are important to understand the LG/ES interaction mechanism.

3.3. *SERS spectra of LG/ES complex*

The SERS spectrum of either α-ES or β-ES cannot be seen on Ag NPs, probably due to the low affinity of the pesticide towards the metal surface. In contrast, intense SERS features of both ES isomers can be seen when the Ag NPs are previously functionalized by the addition of LG (Fig. 3c). It is interesting to note that the detection of the ES was not possible when the above functionalization was made by using other structurally related viologens such as methyl viologen (paraquat) or *N*,*N*′-ethylene-2,2′-bipyridinium (diquat). This is probably due to the larger hydrophobicity afforded by the two acridinium moieties in the central part of LG, thus pointing out that the LG/ES interaction is highly specific.

A study of the influence of the LG concentration on the intensification of ES SERS spectrum revealed that the optimum concentration of LG is 10^{-6} M (Fig. 4). At this concentration the assembler seem to adopt an optimal organization on the metal, which allows the formation of appropriate intermolecular cavities, where the analyte can be hosted (Fig. 5). Indeed, these cavities are similar to the intramolecular ones provided by the cavitands also employed to link analytes [17]. This organization and the formation of such cavities favor the analyte approach to the surface and its SERS enhancement. At higher LG concentrations, a significant compactness of the LG monolayer could occur, thus reducing the possibility of an interaction of the pesticide and its subsequent approach the surface. On the contrary, a lower LG concentration and a decrease in the available binding sites could happen, leading to a dramatic decrease of the SERS signal from the analyte. The SERS spectrum of ES can be seen for a pesticide concentration

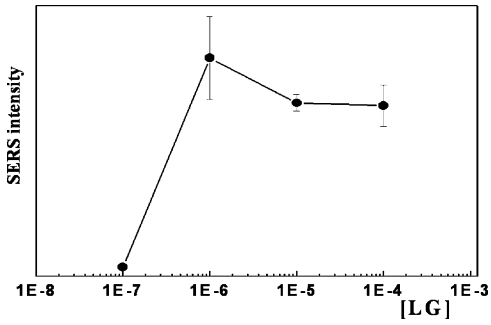

Fig. 4 – SERS intensity of the 400 cm^{-1} ES band at different LG concentrations maintaining the concentration of α-ES at 10^{-4} M. A normalization of the SERS spectra was performed with respect to the Ag–Cl band at 243 cm^{-1}, used as a reference band. In the figure the average values as well as the quadratic standard deviations are displayed.

as low as 10^{-6} M, which corresponds to a limit of detection of 20 ppb.

In addition to the detection of the analyte, by means of its characteristic Raman features, an interesting advantage of sensing methods based on vibrational spectroscopies is the possibility of studying the interaction mechanism with the host molecule. This can be deduced by analysing both the host and the pesticide Raman bands. For the sake of clarity, SERS difference spectra (Fig. 3d and e) were obtained at different concentrations by subtracting the LG SERS spectrum (Fig. 3b). These difference spectra reveal changes in the region below 420 cm^{-1}, indicating a conformational change from the α- to the β-ES isomer upon interaction with the LG-functionalized

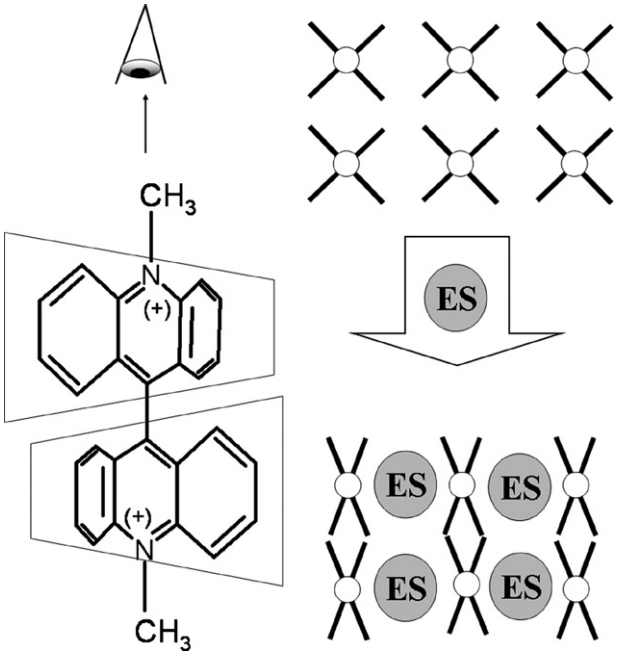

Fig. 5 – Upper view of the intermolecular cavities of LG molecules adsorbed onto the metal surface and the rotation of the acridinium planes taking place once the interaction with α-ES takes place.

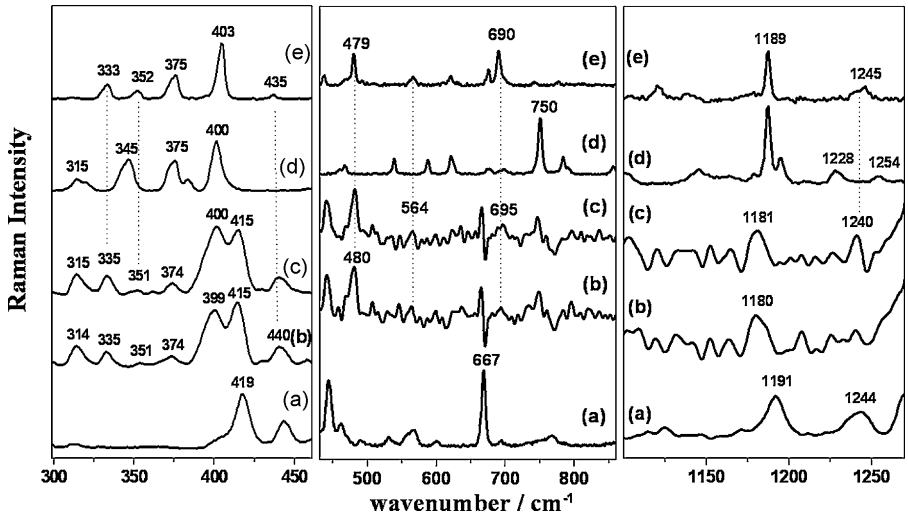

Fig. 6 – Detailed regions of the following Raman and SERS spectra: (a) SERS spectrum of LG (10^{-6} M). (b and c) SERS difference spectra of LG/α-ES complexes at the concentration ratios: 10^{-6} M/10^{-5} M and 10^{-6} M/10^{-4} M, respectively. (d and e) Raman spectra of α-ES and β-ES isomers in the solid state.

metal nanoparticles. Fig. 6 displays in more details the main spectral changes observed upon complexation of α-ES with LG. The existence of an α- to β-isomerization is supported by the fact that a charged environment, as that imposed by LG, mainly stabilises the molecular conformers with the higher dipole moment. This is the case of the β-ES isomer, which dipolar moment is higher than that of the α isomer [43].

The most intense C–Cl stretching band of α-ES at 400 cm^{-1} (Fig. 6d, left panel) undergoes a broadening with the appearance of a shoulder at ca. 397 cm^{-1}. These changes and the relatively high frequency of this band with respect to the other C–Cl bands further support its assignment to the C–Cl stretching of the Cl–C=C–Cl fragment, which is involved in the interaction with LG. Furthermore the SERS spectra reveal bands in the range of the C–Cl deformations: 374, 315, 351 and 335 cm^{-1}, where the latter two are characteristic of the β-isomer.

Another feature that suggest the conformational change from the α- to the β-ES isomer is the weakening of the α-ES characteristic band at 750 cm^{-1} (Fig. 6d, central panel) and the subsequent intensification of β-ES bands at 480, 564 and 695 cm^{-1} (Fig. 6c, central panel).

The C=C stretching mode at 1604 cm^{-1} decreases in intensity or shifts to lower frequency by surface effect overlapping the LG band at 1584 cm^{-1} (Fig. 7, right panel). This is also connected to the pesticide interaction with LG through the Cl–C=C–Cl moiety. We suggest that this interaction may occur by a charge-transfer from the Cl atoms in ES to the N atoms of the acridinium moiety of LG. The CT effect must be enhanced by the presence of the double bond, which donates electric charge, thus decreasing its Raman intensity by a decrease of its polarizability.

Unfortunately, the weak SO_3 stretching band appearing at 1189 cm^{-1} (Fig. 6d, right panel) overlaps the LG band appearing at 1191 cm^{-1} (Fig. 6a, right panel) and a unique band is seen in the SERS of LG/ES complex at 1181 cm^{-1} (Fig. 6b and c, right panel). However, the relative weakness of these modes avoids inferring more deeply on the possible conformational change or interaction of the sulfonic group with the host or the surface. The weak bands appearing at 1254 and 1228 cm^{-1}, seen in the Raman spectrum of the α-ES (Fig. 6d, right panel) can be attributed to the SO_3 group and are also sensitive to the local conformation of the sulfonic ester. In fact, these bands disappear in the β-ES spectrum, appearing a unique band at 1245 cm^{-1} instead. The last band was also observed in the SERS of LG/ES complex at 1240 cm^{-1} (Fig. 6c, right panel), thus supporting again the isomer transition in the LG-functionalized surface. The presence of the sulfonic ester seems to be important in the interaction with LG, as suggests

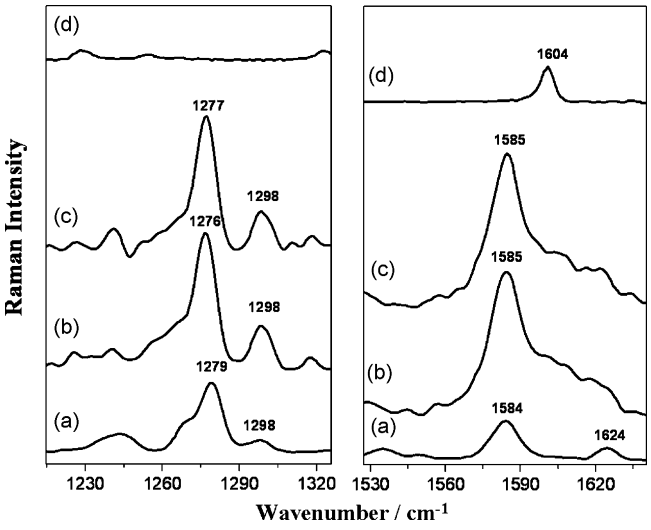

Fig. 7 – Detailed regions of the following Raman and SERS spectra: (a) SERS spectrum of LG (10^{-6} M). (b and c) SERS difference spectra of LG/α-ES complexes at the concentration ratios: 10^{-6} M/10^{-5} M and 10^{-6} M/10^{-4} M, respectively. (d) Raman spectra of α-ES isomers in the solid state.

the fact that no SERS spectrum was obtained from other structurally related pesticides where this group is absent, such as the case of aldrin.

The interaction of ES with the LG dication also induces structural changes on the host which are better seen in Fig. 7. The most evident spectral changes were detected in bands with some contribution from the N atoms. This is the case for instance, of the band at 1584 cm^{-1} (Fig. 7a, right panel), which is attributed to in-plane ring stretching vibrations of the central acridine moiety [44]. The latter band undergoes a marked intensification indicating the formation of a CT complex between LG and ES. Another consequence of this interaction is the disappearance of the 1624 cm^{-1} band. The interaction of ES takes place through the N^+-CH_3 moiety of LG as indicated the shifts of the bands at 1395, 1430 and 1191 cm^{-1}, the ring-breathing band of the acridine moieties at 1036 cm^{-1}, and the band at 668 cm^{-1}, assigned to the δ(CNC) vibration (see difference spectra in Fig. 3d and e). Furthermore, these changes are accompanied by the shift of the vibrations involving the N^+ moiety at 419–415 cm^{-1} (Fig. 6, left panel). All these facts indicate that the interaction of ES takes place through the N atom of LG.

In addition, the interaction of ES with LG induces significant changes on the bands sensitive to the inter-ring angle, i.e. those appearing in the 1200–1300 cm^{-1} region (Fig. 7, left panel). In particular, a marked enhancement of the band at 1298 cm^{-1} is seen, along with a downshift of the δ(C–H) vibration of the acridine ring from 1191 to 1180 cm^{-1} (Fig. 6, right panel). Both facts suggest conformational changes regarding the torsion of both LG rings toward higher coplanarity in order to better accommodate the ligand, as outlined in Fig. 5.

4. Conclusions

Intense SERS features of the pesticide ES at concentrations as low as 10^{-6} M can be seen when the Ag NPs are previously functionalized by the viologen LG. The limit of detection deduced from this technique is 20 ppb. In addition to the fact that the pesticide can be detected at low concentrations, the SERS technique affords valuable information about the interaction mechanism. The charged environment imposed by the colloidal solution and the bis-acridinium dications induce structural changes in the pesticide, which is stabilised in the complex as the β-isomer. Besides, the structure of LG is modified in the presence of the analyte. ES is placed between the lucigenine molecules, inducing a rotation of the acridinium planes and an interaction with the N atom of the central acridinium ring through a charge-transfer complex involving the pesticide Cl–C=C–Cl fragment. The interaction verified between the analyte and the assembler is specific, as other structurally related pesticides such as aldrin are not detected by LG-functionalized NPs. Besides, this interaction allows an approach of the pollutant to the surface leading to the enhancement of its Raman spectrum. The present study affords important information which can be applied in the design of chemical sensor systems of POPs based on the metal nanoparticle functionalization with viologens bearing a large aromatic character.

Acknowledgments

Authors acknowledge projects Fondecyt 1040640 and 1070078 from Conicyt, *Dirección General de Investigación* (*Ministerio de Educación y Ciencia*) project number FIS2006-63065, *Comunidad Autónoma de Madrid* project number S-0505/TIC/0191 MICROSERES, and Proyecto de Cooperación Internacional CONICYT/CSIC 2005-150/2005CL0002 for financial support. L.G. acknowledges CSIC for an I3P fellowship.

REFERENCES

[1] C.M. Niemeyer, Angewandte Chemie-International Edition 40 (2001) 4128.
[2] W.R. Glomm, Journal of Dispersion Science and Technology 26 (2005) 389.
[3] R.F. Aroca, R.A. Alvarez-Puebla, N. Pieczonka, S. Sanchez-Cortez, J.V. Garcia-Ramos, Advances in Colloid and Interface Science 116 (2005) 45.
[4] M.V. Cañamares, J.V. Garcia-Ramos, J.D. Gomez-Varga, C. Domingo, S. Sanchez-Cortes, Langmuir 21 (2005) 8546.
[5] S. Sanchez-Cortes, J.V. Garciaramos, G. Morcillo, Journal of Colloid and Interface Science 167 (1994) 428.
[6] M. Moskovits, Reviews of Modern Physics 57 (1985) 783.
[7] M. Moskovits, Journal of Chemical Physics 69 (1978) 4159.
[8] M.G. Albrecht, J.A. Creighton, Journal of the American Chemical Society 99 (1977) 5215.
[9] F.J. Adrian, Chemical Physics Letters 78 (1981) 45.
[10] D.S. Wang, M. Kerker, Physical Review B 24 (1981) 1777.
[11] S. Sanchez-Cortes, J.V. Garcia-Ramos, Langmuir 16 (2000) 764.
[12] A.M. Alak, T. Vodinh, Analytical Chemistry 59 (1987) 2149.
[13] A.M. Alak, T. Vodinh, Analytica Chimica Acta 206 (1988) 333.
[14] P. Leyton, C. Domingo, S. Sanchez-Cortes, M. Campos-Vallette, J.V. Garcia-Ramos, Langmuir 21 (2005) 11814.
[15] P. Leyton, J.S. Gomez-Jeria, S. Sanchez-Cortes, C. Domingo, M. Campos-Vallette, Journal of Physical Chemistry B 110 (2006) 6470.
[16] P. Leyton, S. Sanchez-Cortes, M. Campos-Vallette, C. Domingo, J.V. Garcia-Ramos, C. Saitz, Applied Spectroscopy 59 (2005) 1009.
[17] P. Leyton, S. Sanchez-Cortes, J.V. Garcia-Ramos, C. Domingo, M. Campos-Vallette, C. Saitz, R.E. Clavijo, Journal of Physical Chemistry B 108 (2004) 17484.
[18] P. Leyton, I. Córdova, P.A. Lizama-Vergara, J.S. Gómez-Jeria, A.E. Aliaga, M.M. Campos-Vallette, E. Clavijo, J.V. García-Ramos, S. Sanchez-Cortes, Vibrational Spectroscopy 46 (2008) 77.
[19] P.M.S. Monk, The Viologens: Physicochemical Properties, Synthesis and Applications of the Salts of 4,4′-Bipyridine, John Wiley & Sons, Chichester, 1998.
[20] X. Liu, K.G. Neoh, E.T. Kang, Langmuir 18 (2002) 9041.
[21] J.M. Zen, C.W. Lo, Analytical Chemistry 68 (1996) 2635.
[22] K. Itaya, H. Akahoshi, S. Toshima, Journal of the Electrochemical Society 129 (1982) 762.
[23] A.H. Ma, Z. Rosenzwieg, Analytical Chemistry 76 (2004) 569.
[24] Z.H. Chen, J.A. Wang, Z.Y. Lin, G.N. Chen, Talanta 72 (2007) 1410.
[25] C. Huber, I. Klimant, C. Krause, O.S. Wolfbeis, Analytical Chemistry 73 (2001) 2097.
[26] J.I. Millan, J.V. Garcia-Ramos, S. Sanchez-Cortes, Journal of Electroanalytical Chemistry 556 (2003) 83.

[27] J.I. Millan, J.V. Garcia-Ramos, S. Sanchez-Cortes, R. Rodriguez-Amaro, Journal of Raman Spectroscopy 34 (2003) 227.
[28] L. Guerrini, Z. Jurasekova, C. Domingo, M. Perez-Mendez, P. Leyton, M. Campos-Vallette, J.V. Garcia-Ramos, S. Sanchez-Cortes, Plasmonics 2 (2007) 147.
[29] S.T. Oh, K. Kim, M.S. Kim, Journal of Physical Chemistry 95 (1991) 8844.
[30] S. Sanchez-Cortes, L. Guerrini, J.V. Garcia-Ramos, C. Domingo, Optica Pura y Aplicada 40 (2007) 235.
[31] United Nations Environment Programme, Environ. Data Report 1993–94, Blackwell Publishers, Oxford, 1993.
[32] R.B. Koch, Chemico-biological Interactions 1 (1969) 199.
[33] L.C. Folmar, Bulletin of Environmental Contamination and Toxicology 19 (1978) 481.
[34] M. Luo, R.P. Bodnaryk, Pesticide Biochemistry and Physiology 30 (1988) 155.
[35] G. Holan, T.H. Spurling, Experientia 30 (1974) 480.
[36] P.N. Saxena, V.D. Gupta, Journal of Applied Toxicology 25 (2005) 39.
[37] H. Maier-Bode, Residue Reviews 22 (1968) 1.
[38] A.S. Nair, R.T. Tom, T. Pradeep, Journal of Environmental Monitoring 5 (2003) 363.
[39] N. Leopold, B. Lendl, Journal of Physical Chemistry B 107 (2003) 5723.
[40] D. Lin-Vien, N.B. Colthup, W.G. Fateley, J.G. Graselli, The Handbook of Infrared and Raman Characteristic Frequencies of Organic Molecules, Academic Press, Boston, 1991.
[41] K. Nakamoto, Infrared and Raman Spectra of Inorganic and Coordination Compounds, Wiley–Interscience, London, 1997.
[42] G. Socrates, Infrared and Raman Characteristic Group Frequencies, John Wiley & Sons, 2004.
[43] D. Mackay, W.Y. Shiu, K.C. Ma, Illustrated Handbook of Physical–Chemical Properties and Environmental Fate of Organic Chemicals, Lewis Publishers, 1997.
[44] R.E. Hester, S. Suzuki, Journal of Physical Chemistry 86 (1982) 4626.